Photoresponsive, amide-based derivative of embonic acid for anion recognition

Natalia Łukasik[a],*, Jarosław Chojnacki[b], Elżbieta Luboch[a], Andrzej Okuniewski[b], Ewa Wagner-Wysiecka[a],*

[a] Department of Chemistry and Technology of Functional Materials, Gdańsk University of Technology, Narutowicza Street 11/12, 80-233 Gdańsk, Poland
[b] Department of Inorganic Chemistry, Faculty of Chemistry, Gdańsk University of Technology, Narutowicza Street 11/12, 80-233 Gdańsk, Poland

A B S T R A C T

The synthesis and ion-binding properties of amide-based derivative of embonic acid and p-aminoazobenzene were described. The new compound was characterized by X-ray structural analysis and spectroscopic methods. Ligand interacts in acetonitrile with Y-shaped anions (benzoates and acetates) and dihydrogen phosphates forming complexes of 1:1 stoichiometry. In more polar DMSO the complexes stoichiometry changes to 2:1 (L:anion). Light-induced trans to cis isomerization was studied. The effect of anions on thermal back isomerization was investigated.

1. Introduction

For many years one of the key areas of research within supramolecular chemistry is the design, synthesis and studies of properties of ion receptors. This interest is connected with vast spectrum of potential applications of such compounds as for instance in development of chemical sensors [1], obtainment of new therapeutic systems enabling ion transport through cell membrane [2], remediation of waters and soils contaminated with radioactive ions [3] and others. One of the conditions of selective recognition of ionic species by molecular receptors is their geometrical molding. In the presence of complementary ion, the host molecule can undergo preorganization to suit better the size and shape of the ion. However, the change of ligand configuration requires energy inputs, which if they exceed the energy of host-guest interactions, cause that additional energy must be supplied to the system. The changes of ligand geometry can be induced by external factors, such as temperature, type and polarity of solvent, electric current flow or pH change. The presence of photoactive groups in ligand structure causes that geometrical changes can be also controlled by electromagnetic radiation [4]. Light, contrary to other external factors, has an inert character and generally ensures that configurational changes occurring upon its action are relatively fast and reversible. Among photoactive compounds derivatives of spiropyran [5], diarylethene[6], and azobenzene [7] can be distinguished. Particular importance have azo compounds as due to their relatively simple synthesis and interesting properties they find diverse applications such

as in digital electronics [8], data recording devices [9], photopharmaceutics [10], and others. Irradiation of azobenzene derivatives with UV or visible light induces configurational changes from almost planar trans (E) isomer to cis (Z) form of geometry resembling the V letter. In darkness or after irradiation with green or blue light the system reequilibrates to thermodynamically more stable trans isomer. Ravoo et al. [11] investigated photoswitching properties of a series of water-soluble arylazopyroles and their host-guest interactions with cyclodextrins. Depending on the type and position of benzene ring substitution, the thermal stability of compounds could be tuned over a broad timescale, from several seconds to days and months. Jurczak and co-workers [12] described anion-controllable cis to trans thermal isomerization of urea-bearing azobenzene receptors in DMSO. The presence of anions accelerated thermal back isomerization, what was explained by electron density transfer from anionic species to the complex resulting in increased repulsion of lone pairs in azo group. The interactions of cis isomer, obtained after solution irradiation, with anions were weaker than for the trans form, what is a consequence of configurational changes and spatial arrangement of binding pocket in both isomers. Light-induced isomerization of azo group was also employed to controlled transport of chloride anions across cell membranes [13]. The described transporters bearing urea units linked via azobenzene spacer were practically inactive in their trans form, however after UV light-triggered isomerization their transport activities were switched on due to more preferable preorganization of the binding sites in cis isomers.

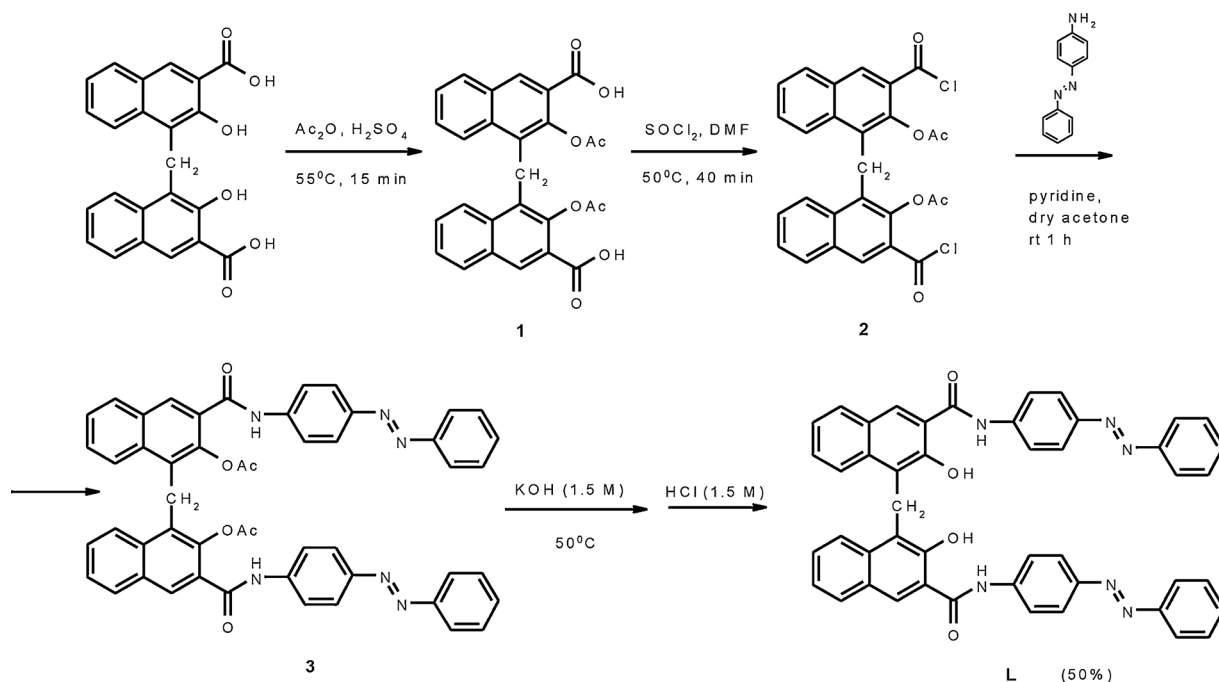Taking all above into consideration, we decided to synthesize amide

---

Fig. 1. Synthesis of amide **L**.

derivative of embonic acid, that due to the presence of hydrogen bond donors: NH or OH groups in its structure should potentially enable anion recognition. The introduction of azo moieties gives a possibility to control ligand configuration and its binding ability by external stimuli *i.e.* light. Complexing properties of the compound were tested in acetonitrile and DMSO.

2. Results and discussion

2.1. Synthesis

Amide **L** was obtained according to synthetic route shown in Fig. 1. The first step was the protection of hydroxyl groups of embonic acid in order to prevent intramolecular hydrogen bonds formation between hydroxyl moieties and *ortho* positioned carboxyl groups [14]. Then acetylated embonic acid (**1**) was used as a substrate for acyl chloride preparation. Condensation of **2** with *p*-aminoazobenzene and subsequent hydrolysis yielded the desired bisamide **L** (total yield 50%). To the best our knowledge (according to Chemical Abstracts) it is the first time when synthesis of this compound is described. Details about synthesis of ligand **L** and its spectral characteristic are included in Supplementary Material (Fig. SM 1–6).

2.2. X-ray structure of L

Compound **L** crystallizes in triclinic system in the space group $P\bar{1}$, Z = 2. Molecular view is presented in Fig. 2. Experimental details and refinement parameters are given in Table 1. Asymmetric unit contains the main organic molecule $C_{47}H_{34}N_6O_4$ which is solvated, due to NH···O hydrogen bridges, by one acetone molecule and by water. Analysis of size of the displacement ellipsoid on O6 indicated that the water molecule has actually site occupation factor of half, so mean chemical formula is given as $C_{47}H_{34}N_6O_4 \cdot C_3H_6O \cdot 0.5(H_2O)$. It means that each two molecules of **L** are solvated by two molecules of acetone and one molecule of water. Both azobenzene fragments are in *trans* form.

One terminal azobenzene group (with N3 N4) was refined as disordered over two positions with occupancies of 0.632(17)/0.368(17). The naphthyl groups form an open, anti-parallel, conformation so no

hydrophilic cavity was created by the molecule itself (naphthyl residues form dihedral angle of 100.52°). Bond lengths and valence angles are within their expected values ranges. Reported size of N3-N4 bond is affected by the disorder and cannot be regarded as precisely determined. Hydrogen bond geometry is given in Table 2. Both hydroxyl groups (O2, O4) form intramolecular hydrogen bonding OH···O with the most proximate C=O groups giving S(6) motif (for graph set notation, see: [15]). The remaining hydrogen bond donors N−H bind acetone and water molecules *via* their O atoms. One branch of the main molecule, solvated by water, has almost coplanar aromatic rings (the one with N1, N2, N6 *etc.*) while the second branch (solvated by acetone) shows distinct deviation from planarity: dihedral angle between the naphthyl C-atoms (C25-C33) and azobenzene C,*N*-atoms (C36-C47) is *ca.* 63.0(1) degree. This part is also affected by disorder of azobenzene group bonded in two orientations. Packing of solvated molecules in crystal is controlled mainly by CH···O hydrogen bonds (see Table 2) and to some extent by stacking interactions, which are not frequent: only two rings have centroid distance less than four angstrems, *i.e.* 3.8760(10) Å for centroids of C6-C11 and C36-C41 (its 1-*x*, -*y*, -*z* equivalent) phenyl rings (Fig. SM 7).

Additional information concerning crystal data can be found in Supplementary Material (Tab. SM 1–5).

2.3. Theoretical calculation

To check what kind of excitation is most responsible for the UV–vis absorption, the TD-DFT calculations were performed *in vacuo* at B3LYP/6-31 + G(d,p) level of theory. Detailed information on the calculation procedure can be found in the experimental part. The strongest oscillator was found at 437.87 nm (excitation energy = 2.8315 eV; oscillator strength = 0.0706). The HOMO-LUMO transition has the greatest contribution to this excitation (Fig. 3).

2.4. Ligand-ion complexation studies

Ion binding studies were carried out using spectroscopic methods in aprotic solvents of different polarity: highly polar DMSO and less polar acetonitrile.

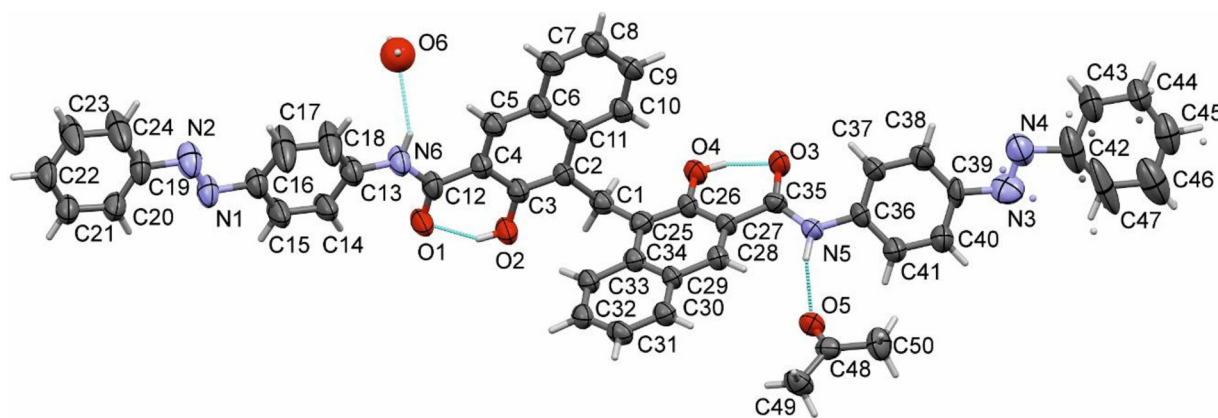Among investigated TBA salts (see Experimental section), changes

Fig. 2. Molecular structure of **L** with atom labelling scheme, displacement ellipsoids drawn at 50% probability level. Atoms of the second disorder part shown as small spheres.

Table 1
Crystal data, data collection and structure refinement details for **L**.

Crystal data	
Chemical formula	$C_{47}H_{34}N_6O_4 \cdot C_3H_6O \cdot 0.5(H_2O)$
M_r	813.89
Crystal system, space group	Triclinic, $P\bar{1}$
Temperature (K)	120
a, b, c (Å)	8.0814 (12), 12.020 (2), 22.340 (6)
α, β, γ (°)	96.510 (19), 94.019 (18), 107.976 (14)
V (Å^3)	2038.1 (8)
Z	2
Radiation type	Mo $K\alpha$
μ (mm^{-1})	0.09
Crystal size (mm)	0.28 × 0.04 × 0.03
Data collection	
Diffractometer	STOE *IPDS* 2 T diffractometer
Absorption correction	none
No. of measured, independent and observed [$I > 2\sigma(I)$] reflections	15151, 7166, 2781
R_{int}	0.129
$(\sin\theta/\lambda)_{max}$ (Å^{-1})	0.595
Refinement	
$R[F^2 > 2\sigma(F^2)]$, $wR(F^2)$, S	0.111, 0.360, 1.01
No. of reflections	7166
No. of parameters	598
No. of restraints	33
H-atom treatment	H atoms treated by a mixture of independent and constrained refinement
$\Delta\rangle_{max}, \Delta\rangle_{min}$ (e Å^{-3})	0.40 −0.35

Table 2
Hydrogen-bond geometry (Å, °) for **L**.

D—H···A	D—H	H···A	D···A	D—H···A
N5—H5···O5	0.88	2.03	2.889 (7)	164
N6—H6···O6	0.88	2.3	3.078 (16)	148
O2—H2···O1	0.84	1.77	2.525 (6)	149
O4—H4···O3	0.84	1.85	2.583 (7)	145
O4—H4···O3^i	0.84	2.64	3.092 (6)	116
C14—H14···O1	0.95	2.35	2.917 (9)	118
C15—H15···O1^{ii}	0.95	2.56	3.411 (9)	149
C18—H18···O2^{iii}	0.95	2.59	3.221 (11)	124
C18—H18···O6	0.95	2.5	3.18 (2)	128
C20—H20···O2^{ii}	0.95	2.61	3.512 (8)	158
C38—H38···O6^{iv}	0.95	2.54	3.368 (17)	146
O6—H6*B*···N4^{iv}	0.82 (2)	2.59 (15)	3.06 (2)	118 (14)
N5—H5···O5	0.88	2.03	2.889 (7)	164
N6—H6···O6	0.88	2.3	3.078 (16)	148
O2—H2···O1	0.84	1.77	2.525 (6)	149
O4—H4···O3	0.84	1.85	2.583 (7)	145
O4—H4···O3^i	0.84	2.64	3.092 (6)	116
C14—H14···O1	0.95	2.35	2.917 (9)	118
C15—H15···O1^{ii}	0.95	2.56	3.411 (9)	149
C18—H18···O2^{iii}	0.95	2.59	3.221 (11)	124
C18—H18···O6	0.95	2.5	3.18 (2)	128
C20—H20···O2^{ii}	0.95	2.61	3.512 (8)	158
C38—H38···O6^{iv}	0.95	2.54	3.368 (17)	146
O6—H6*B*···N4^{iv}	0.82 (2)	2.59 (15)	3.06 (2)	118 (14)

in absorption spectra of **L** were observed in the presence of acetates, benzoates, dihydrogen phosphates and fluorides. Spectral changes upon titration with TBA salts in acetonitrile are exemplified with titration trace for benzoates and fluorides in Fig. 4. Spectral changes upon titration with tetra-*n*-butylammonium acetate and dihydrogen phosphate are shown in Figure SM 8. Similarities in spectra upon titration with benzoates, acetates, and dihydrogen phosphates may indicate similar nature of the interactions with the host molecule **L**. Molar ratio plots obtained from titration experiments at 430 nm suggest 1:1 complex formation in acetonitrile. Different character of changes was observed in spectra registered upon titration with tetra-*n*-butylammonium fluoride (Fig. 4b). No clear isosbestic point can imply that more than one equilibrium under measurement conditions exists. Molar ratio plots obtained from spectrophotometric titration point out formation of species of 1:2 stoichiometry (**L**: TBAF). It can indicate stepwise deprotonation of the amide **L**. To suppress potential ligand deprotonation, titration experiments with TBAF were carried out in the presence of

acetic acid [17]. Changes in UV–vis spectra in the presence of acid are less significant than in neutral acetonitrile, but still observable. This can suggest that ligand-ion interaction may take place in the system even in the presence of highly basic anions (Fig. SM 9). Opposite to pure acetonitrile in acetic acid environment complexes of sandwich type (2:1, **L**: TBAF) are formed, what is supported by the molar ratio plots obtained from titration experiments.

From spectrophotometric titrations the values of stability constant (logK) for complexes of **L** with anions were estimated in pure acetonitrile and in the presence of acetic acid (Table 3). In pure acetonitrile, stability constant values of 1:1 complexes of **L** with carboxylates are higher than with tetrahedral dihydrogen phosphates pointing out the higher affinity of **L** towards Y-shaped anions. The highest value of stability constant, for 1:1 complexes, was obtained for **L**-PhCOO$^-$. Detection limit for benzoate anions determined from spectrophotometric measurements is 3.57×10^{-7} mol/dm^3.

From spectrophotometric titrations carried out in more polar DMSO it can be concluded that in this solvent amide **L** forms 2:1 (L:A) type complexes with anions. As an example spectral changes registered in experiments with dihydrogen phosphates and benzoates are shown in Fig. 5. In this case, ligand shows the strongest affinity towards dihydrogen phosphate anions (Table 4).
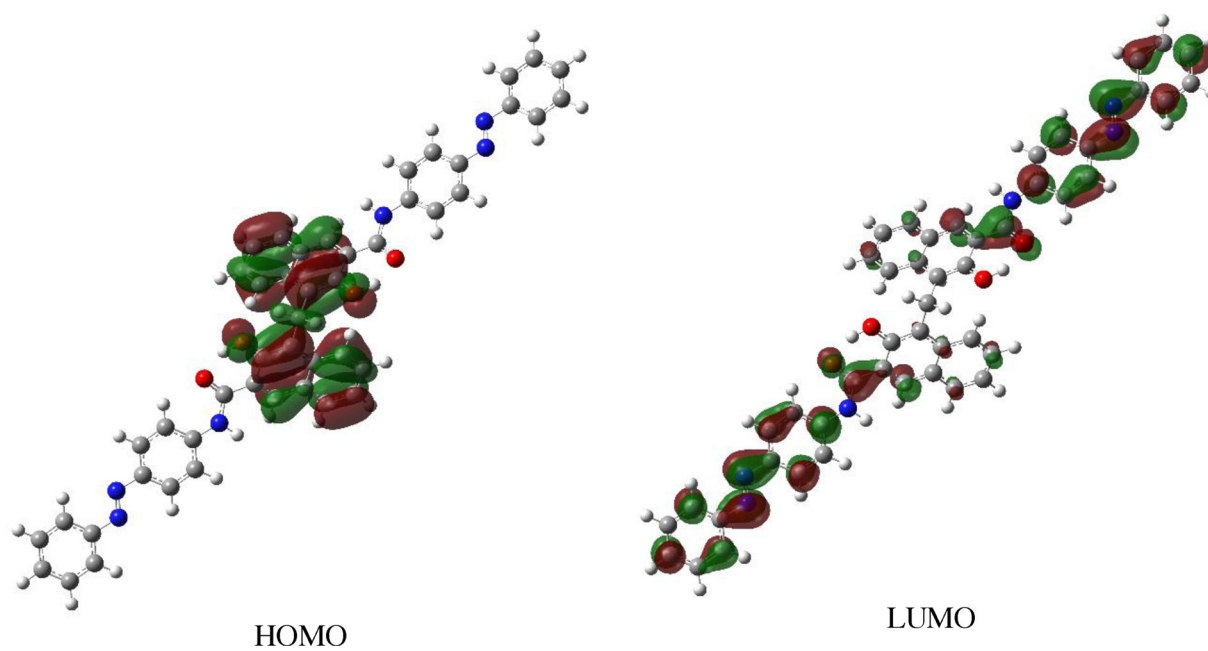
HOMO   LUMO

Fig. 3. HOMO and LUMO molecular orbitals visualized using GaussView 5.0.9 [16].
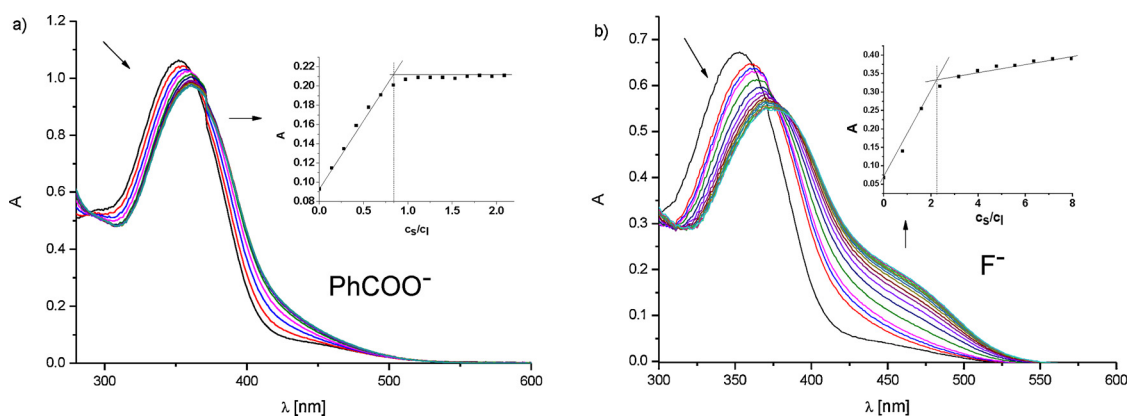

Fig. 4. Spectral changes observed upon titration of the ligand solution with: a) tetra-*n*-butylammonium benzoate ($c_L = 2.17 \times 10^{-5}$ mol/dm^3, $c_s = 0$–4.70×10^{-5} mol/dm^3), inset molar ratio plot at 430 nm; b) tetra-*n*-butylammonium fluoride ($c_L = 1.32 \times 10^{-5}$ mol/dm^3, $c_s = 0$–1.89×10^{-4} mol/dm^3), inset molar ratio plot at 430 nm in acetonitrile.

Table 3

Stoichiometry (L:A) and values of stability constants (logK) for ligand **L** complexes with anions (in the form of TBA salts) in pure acetonitrile and * in the presence of acetic acid (20-fold molar excess in relation to ligand concentration).

Stoichiometry (L:A)	PhCOO$^-$	AcO$^-$	H$_2$PO$_4^-$	F$^-$*
1:1	7.09 ± 0.05	6.64 ± 0.01	5.32 ± 0.04	
2:1				9.87 ± 0.50

Changes observed in UV–vis spectra upon titration with tetra-*n*-butylammonium fluoride are similar to these registered in acetonitrile. Taking into account strongly basic character of fluoride in highly polar DMSO, ligand deprotonation can be here considered. Spectral changes registered upon titrations with TBAF in DMSO in the presence of acetic acid point out the possibility of host-guest interactions (Fig. SM 10). It was found that under measurement conditions 2:1 type complexes (L:A) are formed (Table 4).

Complex formation with anions was also proved by ^{1}H NMR experiments. In ^{1}H NMR spectrum of complex of **L** with benzoates the shift of OH and NH proton signals to higher ppm values in comparison

to the free ligand spectrum is observed. It indicates that in complex formation hydrogen bonds can be involved (Fig. 6). Double signals of unequal intensity seen in the **L**-PhCOO$^-$ spectrum may suggest different involvement of particular protons in interactions with the anion. This may mean that benzoate anion is bound in unsymmetrical manner by the ligand molecule or that complexation of anion triggers isomerization of ligand. In comparison to the free ligand spectrum majority of aromatic protons signals of **L** are shifted to lower ppm values in the presence of the anionic guest. Signals corresponding to aromatic protons of guest, seen in the spectrum of "free" salt at 7.20 and 7.80 ppm (Fig. SM 11), in the complex spectrum are shifted to higher ppm values (seen as overlapping signals at around 7.55 and 7.95 ppm).

The comparison of FTIR spectra of **L**-PhCOO$^-$ complex and the free ligand indicates that the most significant changes are observed in the range of the I amide band (C=O), which in the spectrum of free ligand is observed at 1652 cm^{-1} (Fig. SM 12). In the complex spectrum the band in this region becomes flat. Double, weakly separated bands observed in the spectrum of ligand at around 1440 cm^{-1}, that can be ascribed to C−N stretching and O−H bending vibrations, in the complex spectrum are seen as one sharp band shifted to 1453 cm^{-1}. Additionally, well observable changes in the range 1330−1200 cm^{-1}
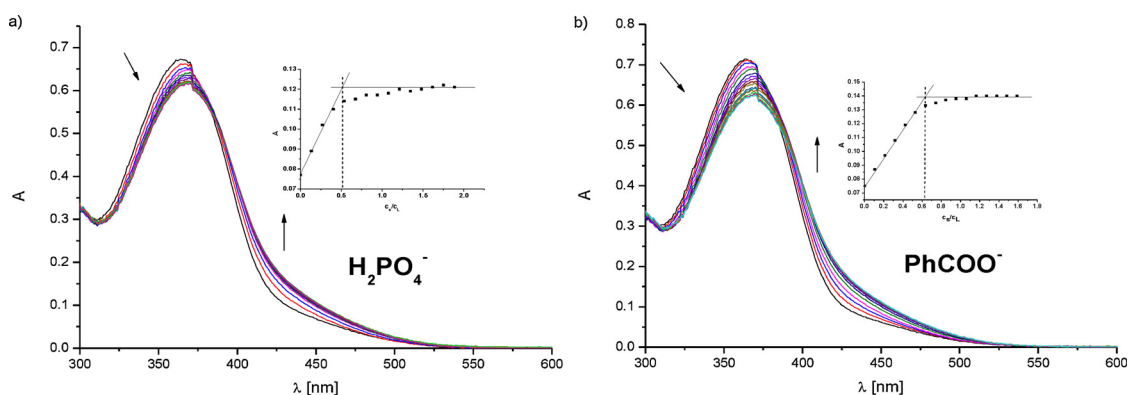
Fig. 5. Spectral changes registered upon titration of **L** ($c_L = 1.81 \times 10^{-5}$ mol/dm³) solution with a) tetra-*n*-butylammonium dihydrogen phosphate ($c_s = 0–3.31 \times 10^{-5}$ mol/dm³); b) tetra-*n*-butylammonium benzoate ($c_s = 0–2.78 \times 10^{-5}$ mol/dm³) in DMSO. Inset: molar ratio plot at 440 nm.

Table 4
Values of stability constants (logK) for ligand **L** complexes (2:1, L:A) with anions (in the form of TBA salts) in pure DMSO and * in the presence of acetic acid (20-fold molar excess in relation to ligand concentration).

Stoichiometry (L:A)	$H_2PO_4^-$	$PhCOO^-$	AcO^-	F^- *
2:1	11.46 ± 0.40	10.46 ± 0.13	10.29 ± 0.77	11.42 ± 0.06

corresponding to ν(C−O) and δ(N−H) out-of-plane vibrations, may indicate that amide and hydroxyl groups of ligand are involved in complex formation, what is supported by ¹H NMR experiments. The presence of benzoate anions influences also on the shape of bands in the region of γ(C−H)$_{ar}$ out-of-plane and ω(N−H) out-of-plane bands ($600 − 800$ cm^{-1}).

¹H NMR spectra were registered also in the presence of dihydrogen phosphates (Fig. SM 13). Addition of 0.5 equivalent of the salt in relation to the ligand concentration caused broadening of all signals and loss of their multiplicity. Signals of OH and NH protons are doubled. It may suggest that under measurement conditions an equilibrium mixture exists and perhaps two forms of the ligand molecule are present. In the presence of equimolar amount of dihydrogen phosphates solution the signals are sharp pointing out that the equilibrium is reached. Again, as in the case of benzoate ions, some of aromatic protons signals are doubled and shifted to lower values of ppm. The OH and NH signals are shifted downfield suggesting the complex formation *via* hydrogen interactions.

Similar character of changes is observed in the spectrum of **L**-F⁻ (Fig. SM 14). Here also, as in the case of benzoate and dihydrogen phosphate ions, NH and OH signals are shifted to higher ppm values pointing out that the main process occurring between ligand and fluoride anions is host – guest complexation. Observed in UV–vis
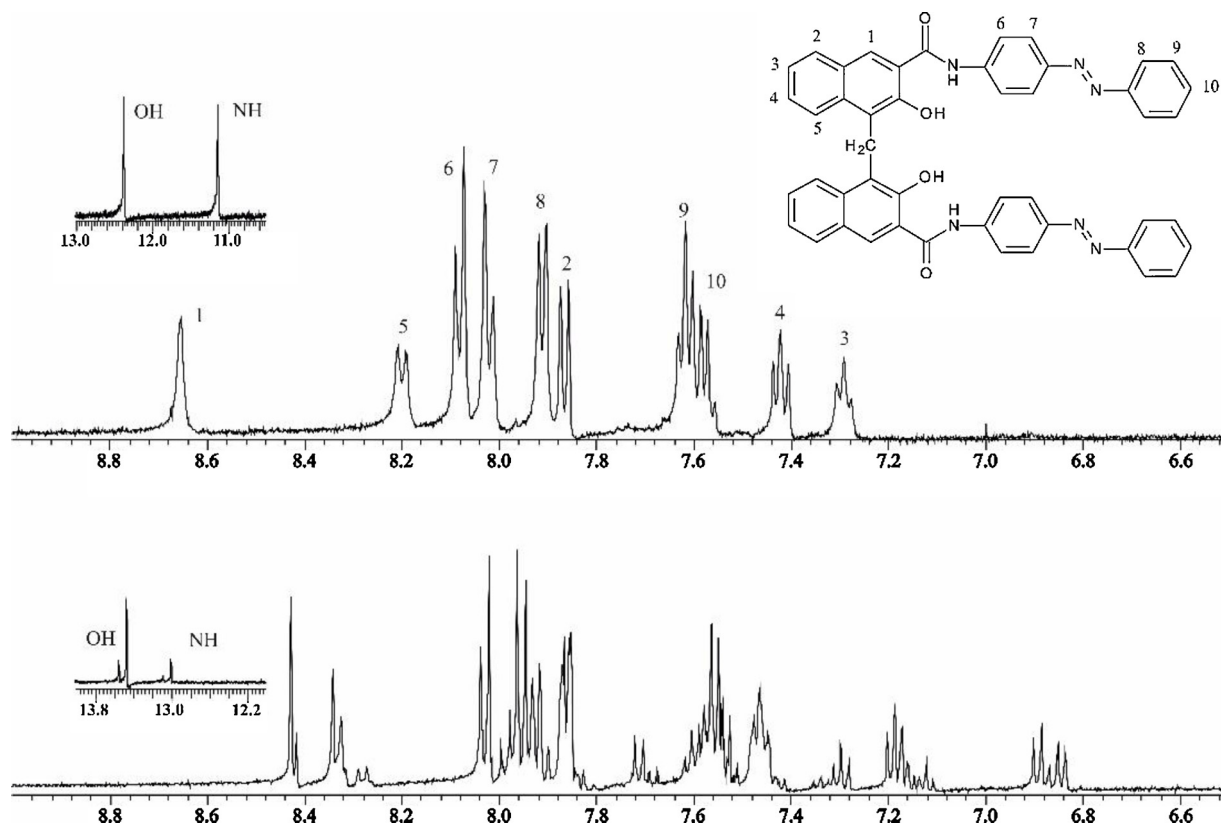

Fig. 6. The comparison of partial ($6.4 − 14$ ppm) ¹H NMR spectra of the free ligand **L** (top) and its 1:1 complex with tetra-*n*-butylammonium benzoate in DMSO-d_6.
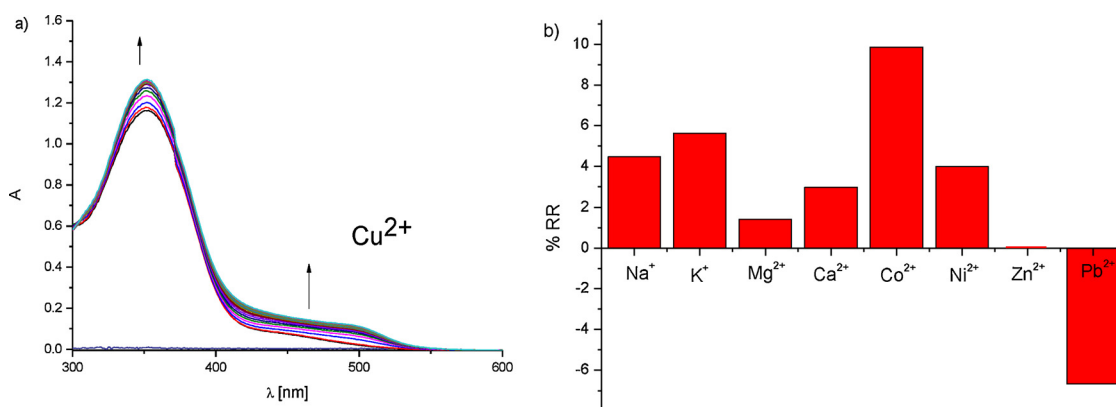
Fig. 7. a) Spectral changes observed upon titration of the ligand solution ($c_L = 2.17 \times 10^{-5}$ mol/dm^3) with copper(II) perchlorate ($c_s = 0$–5.21×10^{-5} mol/dm^3) in acetonitrile; b) The influence of metal cations (10-fold molar excess in relation to copper(II) perchlorate) on the spectrophotometric response of **L** solution ($c_L = 1.82 \times 10^{-5}$ mol/dm^3) in acetonitrile towards copper(II) perchlorate ($c_s = 1.81 \times 10^{-5}$ mol/dm^3), $\lambda = 475$ nm.

studies ligand deprotonation, in ^{1}H NMR experiments is suppressed due to higher concentration of host and guest. Additional evidence of complex formation rather than deprotonation is a lack of triplet ascribed to [HF$_2$]$^-$ adduct at around 16 ppm [18]. Similarly to changes observed in the presence of benzoate and dihydrogen phosphate ions, in the **L**-F$^-$ spectrum additional signals are observed in the region of aromatic proton signals, however their intensity is here much lower (c.a. 10-times as estimated on the basis of integrals).

Among tested metal cation (see Experimental section) changes in UV–vis spectra in acetonitrile were observed only in the presence of copper(II) perchlorate (Fig. 7a). According to molar ratio plots 1:1 type complexes are created under measurement conditions.

Stability constant of 1:1 complex of **L** with copper salt was determined as logK 5.04 ± 0.12. Selectivity of **L** towards copper(II) was estimated as %RR (Fig. 7b). Among tested metal cations the most significant influence on spectrophotometric response of ligand **L** towards copper(II) cations have cobalt(II) and lead(II) cations, however this effect is lower than 10% of relative response. The influence of sodium, magnesium, calcium, nickel(II), and zinc cations is within the measurement error, *i.e.* ± 5% [19], what makes this effect insignificant. Change of solvent to more polar DMSO made ligand-copper(II) interaction studies impossible as it this highly competitive environment no spectral changes in the ligand solution upon addition of copper(II) perchlorate were observed.

2.5. Photoisomerization studies

Due to the presence of two azo groups the compound **L** may potentially exists in three forms: as *trans, trans* (*E,E*) and *trans, cis* (*E, Z*) and *cis, cis* (*Z, Z*) isomer. The photoisomerization process was studied for ligand solution in DMSO. In UV–vis spectrum registered upon ligand irradiation with UV light ($\lambda = 365$ nm) two isosbestic points are observed, what points out that only one process occurs: *trans* to *cis* isomerization. After 6 min of UV-irradiation hypo- and hipsochromic shift of the $\pi \rightarrow \pi^*$ band is seen until a photostationary state is reached what is characteristic for photoismerization of azo compounds (Fig. SM 15) [20]. The band attributed to $n \rightarrow \pi^*$ transition is poorly separated from the $\pi \rightarrow \pi^*$ band and upon irradiation a gentle hyperchromic effect for it is observed. According to the graphical method UV-induced isomerization is a reaction of the first order (Fig. SM 16). According to DSL experiments ligand solution contains particles of around 1 nm size. Upon light-triggered isomerization particles of bigger size *i.e.* around 1540 nm appear. In emission spectra of **L** registered before and after UV-irradiation, a decrease of fluorescence intensity is observed (Fig. SM 17). This effect can be connected with the loss of planarity of **L** molecule upon *trans* to *cis* isomerization. Taking into account DSL results it may be also assumed that upon irradiation aggregates are formed that

cause fluorescence quenching. The process is reversible after heating sample at 50 °C in darkness. In UV–vis spectrum of *Z*-enriched mixture a batho- and hyperchromic effect of the $\pi \rightarrow \pi^*$ band is observed (Fig. SM 18a). According to the graphical method the thermal back reaction is the first order process with half-life time of 22 min (Fig. SM 18b). Spectral characteristic of both isomers is presented in Table 5.

In the ^{1}H NMR spectrum registered after irradiation of **L** solution, additional signals corresponding to *Z* form are seen (Fig. 8). The observed upfield shifts of aromatic (for instance $\Delta \delta_8 = 1.03$ ppm) and NH protons ($\Delta \delta_{NH} = 0.24$ ppm) point out a characteristic shielding effect of overlapping phenyl rings of the *cis* form [21]. According to observed changes it was concluded that two form are present in the mixture. After 1.5 h of irradiation with UV light the concentration of *Z* form in the mixture was estimated as 16%.

Two doublets seen at around 6.9 ppm in the spectrum of UV-irradiated ligand solution are also observed in the spectrum of **L** in the presence of tested anions (Fig. 6, SM 13–14). This may suggest that upon anion binding the isomerization of ligand takes place. In the presence of benzoate and dihydrogen phosphate the content of *Z* form was estimated at around 4% and 9% respectively, whereas in the case of fluoride anions it was lower: c.a. 1%. Thus the affinity of the *Z* isomer towards anions was studied. The presence of selected anionic species that interact with **L** (without irradiation), slows down the rate of thermal reisomerization (Table 6). For the sake of comparison, chloride anions, that do not interact with **L** in DMSO (no spectral changes were observed), speed up thermal back reaction of *Z*-enriched mixture, probably due to the increased repulsion on the N=N group being a consequence of electron density transfer from chloride anion to the complex. In UV–vis spectrum of *Z*-enriched mixture changes are observed in the presence of phosphate, acetate and dihydrogen phosphate anions indicating host-guest interactions between the *Z* form and anions (Fig. SM 19). According to the spectrophotometric titrations the most probable model binding, under measurement conditions, is 1:1 type for complexes with benzoate, acetate and dihydrogen phosphate ions (Fig. 9). UV irradiation-trigger change of complex stoichiometry is probably an effect of different position of binding sites affected by isomerization of azo groups. On the basis of obtained data the stability

Table 5
Spectroscopic data of *E* and *Z* isomers of **L** in DMSO, including absorbance maxima (λ_{max}), separation for the $\pi \rightarrow \pi^*$ transition (Δ), molar extinction coefficients (ε) determined at the irradiation wavelength.

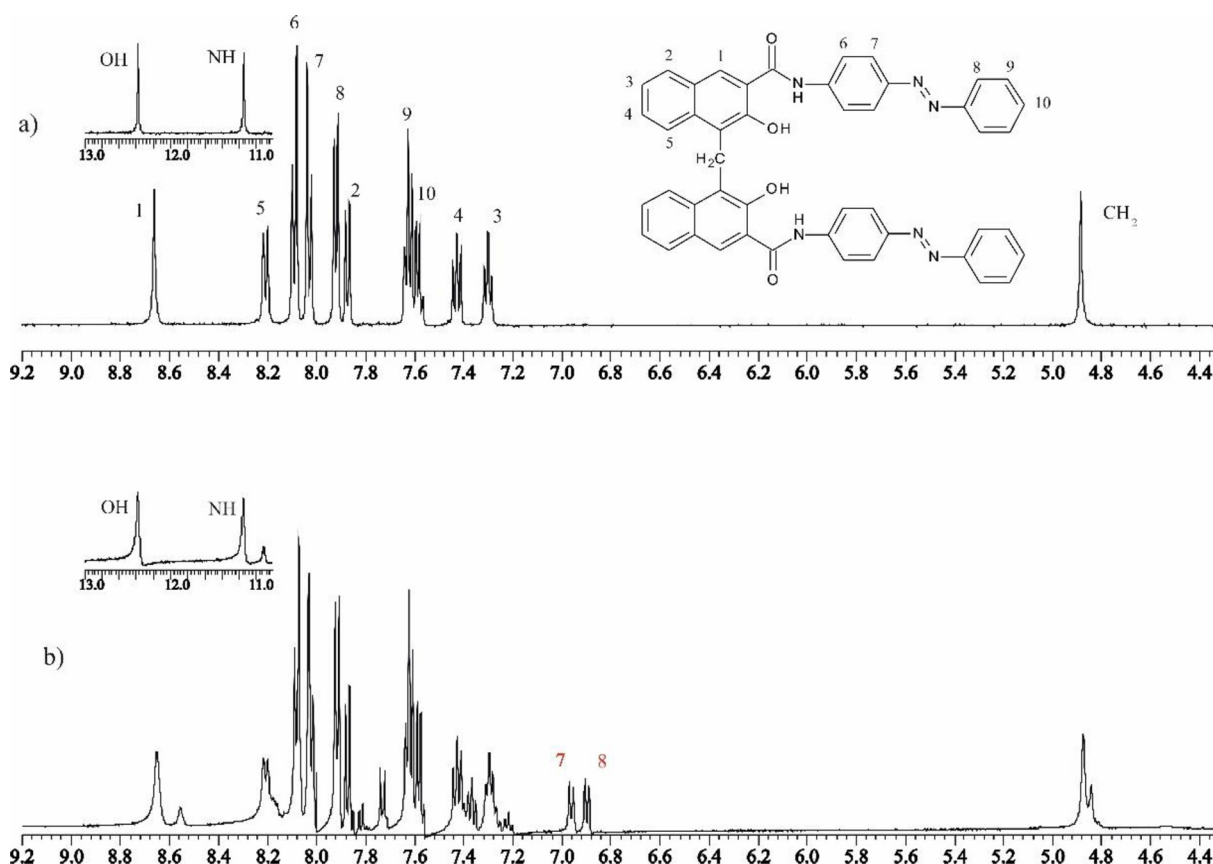| λ_{max} [nm]		Δ [nm]	ε [dm^3 mol^{-1} cm^{-1}]	
E	*Z*		*E*	*Z*
368	338	30	4.7×10^4	2.6×10^4

Fig. 8. Comparison of partial (4.4–13 ppm) ^{1}H NMR spectra of **L** a) before irradiation b) and *Z*-enriched mixture of **L** (bottom) in DMSO-d_6 obtained after 1.5 h of irradiation with UV light ($\lambda = 365$ nm).

Table 6
Kinetic data of *Z→E* thermal isomerization in the presence of equimolar amount of selected tetra-*n*-butylammonium salts. Values of stability constant (logK) determined for 1:1 complexes of *Z*-enriched mixture with selected anions in DMSO, – not determined due to lack of interaction.

	PhCOO$^-$	AcO$^-$	H$_2$PO$_4^-$	Cl$^-$
$\tau_{1/2}$ [min]	32	38	37	4
logK	4.54 ± 0.20	3.41 ± 0.36	4.12 ± 0.02	–

constant values were estimated and presented in Table 6.

3. Conclusions

Described for the first time amide **L** being derivative of embonic acid interacts with benzoate, acetate, dihydrogen phosphate and fluoride ions in acetonitrile and DMSO. Among tested metal cations, the compound selectively binds copper(II) perchlorate in acetonitrile. The highest affinity of ligand, in the case of 1:1 complexes in acetonitrile, was determined for Y-shaped anions, which are bound *via* hydrogen bonds of NH and OH groups. In more polar solvent the stoichiometry of species changes as 2:1 (**L**: anion) complexes dominate under measurement conditions. UV light irradiation of ligand solution induces *trans* to
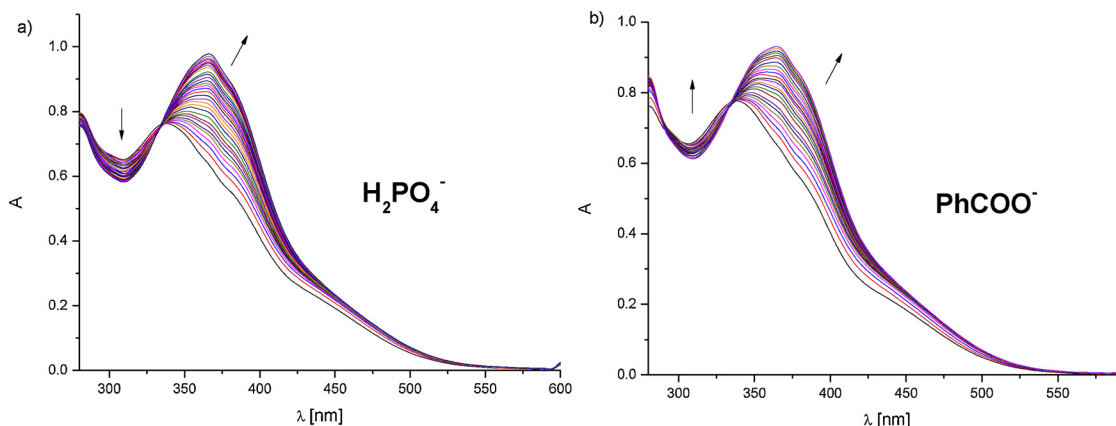

Fig. 9. Changes in UV–vis spectrum of *Z*-enriched mixture of **L** solution ($c_L = 2.44 \times 10^{-5}$ mol/dm^3) in the presence of a) tetra-*n*-butylammonium dihydrogen phosphate ($c_s = 0$–1.77×10^{-4} mol/dm^3); b) tetra-*n*-butylammonium benzoate ($c_s = 0$–1.65×10^{-4} mol/dm^3) in DMSO.

cis isomerization. The process is reversible by heating solution in darkness. The speed of thermal back reaction can be controlled by anionic species. The presence of acetate, benzoate and dihydrogen phosphate ions in irradiated ligand mixture extends half-live times of thermal back isomerization what is an effect of host-guest interaction of *Z* isomer with tested anions. However, chloride anions, in the case of which no interactions with ligand were observed, accelerate this process.

4. Experimental

4.1. General

All chemicals of the highest available purity were purchased from commercial sources and used without further purification. The reaction progress was monitored by TLC using aluminum sheets covered with silica gel 60F$_{254}$ (Merck). ^{1}H NMR and ^{13}C spectra were recorded on Varian Unity Inova 500 apparatus at 500 MHz and at 125 MHz respectively. Chemical shifts are reported as δ [ppm] values in relation to TMS. FTIR spectra (KBr pellets) were taken on a Nicolet iS10 apparatus. UV–vis titrations were carried out in acetonitrile (LiChrosolv MERCK) and DMSO (POCH) using an UNICAM UV 300 spectrophotometer. For spectrophotometric measurements 1 cm quartz cuvettes were used. UV irradiation experiments were carried out in a prototype photoreactor designed by Dariusz Wysiecki M.Sc.,Eng. and constructed in cooperation with Enviklim Company (Poland). The reactor is equipped with 3 UVA diode arrays ($2 \times$ UV-D6565-4LED, 40 W and $1 \times$ UV-D6565-15LED, 150 W, $\lambda = 365-370$ nm). The particle size distribution of ligand solution before and after UV-light irradiation was measured by DSL (dynamic light scattering) method using a Zetasizer Nano apparatus (Malvern Instruments Ltd).

4.2. X-ray single crystal structural analysis

Single crystals of **L** were obtained by slow evaporation of acetone from solution ($c_L \sim 10^{-3}$ mol/dm^3) at room temperature. X-ray diffraction data were collected on an IPDS 2 T dual-beam diffractometer (STOE &Cie GmbH, Darmstadt, Germany) at 120 K with Mo-K$_\alpha$ radiation of a microfocus X-ray source (GeniX 3D Mo High Flux, Xenocs, Sassenage, France, 50 kV, 1.0 mA, $\lambda = 0.71073$ Å). The crystal was thermostated in nitrogen steam at 120 K using CryoStream-800 device (Oxford, CryoSystem, UK). Data reduction was performed by STOE *X-AREA* software [22]. The structure was solved and refined by *SHELXS* [23] and *SHELXL2014* [24] programs. Molecular graphics were obtained with the use of Olex2 software [25]. Crystal data, data collection and structure refinement details are summarized in Table SI 1. All specimens had very weak diffracting power, therefore long frame exposure time (4 min) was applied. Despite rather low resolution, electron density maps give molecular structure of reasonable quality. All atoms accept hydrogen were refined using anisotropic model. For isotropic hydrogen atoms U$_{iso}$ was fixed to be 1.2 times of U$_{iso}$ heavy atoms for CH$_2$, CH and NH groups, 1.5 times of U$_{iso}$ of heavy atoms for CH$_3$ and OH groups. OH hydrogen atoms were refined with the O$-$H distance constrained to 0.82(2)Å.

4.3. Theoretical calculation

The starting structure of **L** was taken from crystallographic data. As one of the azo-fragments of the molecule is disordered over two positions the more symmetric isomer (approx. C_2 point group) was selected. Optimization of **L** was performed *in vacuo* using Gaussian 09 W rev. D.01 [26] at B3LYP/6-31 + G(d,p) level of theory with D3 dispersion correction by Grimme. The vibrational analysis shows that there are no negative frequencies, so the optimized structure is in a local minimum of the potential energy surface. Later on, excited states were calculated using time-dependent DFT at the same level of theory. Calculations were performed within PL-Grid Infrastructure.

4.4. Ligand-ion interaction studies

Complexation studies were performed by UV–vis titration of the ligand solution in acetonitrile or DMSO with the respective metal perchlorates (for metal cations complexation studies) or tetra-*n*-butylammonium (TBA) salts (for anions complexation studies). In studies TBA salts (halides, nitrate(V), hydrogen sulfate, thiocyanate, perchlorate, *p*-toluenesulfonate, benzoate, acetate, dihydrogen phosphate) and metal perchlorate salts (Li$^+$, Na$^+$, K$^+$, Mg^{2+}, Ca^{2+}, Sr^{2+}, Ba^{2+}, Co^{2+}, Ni^{2+}, Cu^{2+}, Pb^{2+}, Zn^{2+}) were used. The stock solutions of ligands ($\sim 10^{-4}$ M) and metal perchlorates or TBA salts ($\sim 10^{-2}$ mol/dm^3) were prepared by weighing the respective quantities of them and dissolving in pure acetonitrile or DMSO in volumetric flasks. Titrations were carried out in a quartz cuvette with path length of 1 cm with starting volume of the ligand solution equal to 2.3 mL. To suppress deprotonation process, titrations were also carried out in the presence of acetic acid (20-fold molar excess in relation to ligand concentration). On the basis of experimental data the stability constant values were determined using OPIUM software [27]. The detection limits (LOD) were calculated from plots A = f (concentration of TBA salt) using equation:

$$LOD = \frac{3\sigma}{K}$$

Where σ is the standard deviation of the blank and K is the slope of the linear calibration range. The influence of selected interfering metal cations on spectrophotometric copper(II) recognition by amide **L** in acetonitrile is presented as relative response (%RR):

$$\%RR = \frac{A - A_0}{A_0} \times 100\%$$

where A_0 is the absorbance of the ligand solution in the presence of copper(II) perchlorate at fixed concentration (1 equivalent) and A is the absorbance recorded after addition to the ligand solution containing the analyte of interfering metal cation (as perchlorate salt) in the concentration 10-times higher than the analyte.

4.5. Complex preparation for spectroscopic studies

Samples for ^{1}H NMR analysis were prepared by dissolving of **L** (0.007 mmol) and tetra-*n*-butylammonium dihydrogen phosphate, benzoate or fluoride (0.007 mmol) in 15 ml of acetone. The resulting mixture was stirred until complete dissolution. After solvent evaporation under reduced pressure, the respective sample was dissolved in DMSO-d_6 and its spectrum was registered. Similar procedure (without dissolution in DMSO-d_6) was applied for complexes prepared for FTIR analysis.

4.6. Photoisomerization studies

UV irradiation experiments were carried out in a quarz cuvette (l =1 cm) in DMSO. The progress of photoisomerization was monitored by UV–vis spectrophotometry and ^{1}H NMR spectroscopy. For UV–vis spectrophotometric experiments ligand solution of c $\sim 10^{-5}$ mol/dm^3 was prepared. In ^{1}H NMR measurements more concentrated solution (c $\sim 10^{-3}$ mol/dm^3) was used. The reverse isomerization was led in darkness at 50 °C. The stability constant values for anion complexes were determined on the basis of spectrophotometric titration of irradiated ligand solution with the selected tetra-*n*-butylammonium salts.

The authors declare that the manuscript has not been published before and it is not currently under consideration for publication in any other journal. The publication of the manuscript has been approved by all authors. Authors declare that the manuscript, after publishing in Journal of Photochemistry and Photobiology A: Chemistry, will not be

published elsewhere in the same form in English or any other language without the written consent of the copyright-holder.

On behalf of all authors of the manuscript;" Photoresponsive, amide-based derivative of embonic acid for anion recognition" written by N. Łukasik, J. Chojnacki, E. Luboch, A. Okuniewski and E. Wagner-Wysiecka, I declare no conflict of interest.

Acknowledgments

Appendix A. Supplementary data

Supplementary material related to this article can be found, in the online version, at doi:https://doi.org/10.1016/j.jphotochem.2019.112307.

References

[1] a) N. Pankratova, M. Cuartero, L.A. Jowett, E.N.W. Howe, P.A. Gale, E. Bakker, G.A. Crespo, Fluorinated tripodal receptors for potentiometric chloride detection in biological fluids, Biosens. Bioelectron. 99 (2018) 70–76;
b) N. Łukasik, E. Wagner-Wysiecka, A. Małachowska, Iron(III)-selective materials based on a catechol-bearing amide for optical sensing, Analyst 144 (2019) 3119–3127.

[2] a) V. Soto-Cerrato, P. Manuel-Manresa, E. Hernando, S. Calabuig-Fariñas, A. Martínez-Romero, V. Fernández-Dueñas, K. Sahlholm, T. Knöpfel, M. García-Valverde, A.M. Rodilla, E. Jantus-Lewintre, R. Farràs, F. Ciruela, R. Pérez-Tomás, R. Quesada, Facilitated anion transport induces hyperpolarization of the cell membrane that triggers differentiation and cell death in cancer stem cells, J. Am. Chem. Soc. 137 (2015) 15892–15898;
b) N. Busschaert, S.-H. Park, K.-H. Baek, Y.P. Choi, J. Park, E.N.W. Howe, J.R. Hiscock, L.E. Karagiannidis, I. Marques, V. Félix, W. Namkung, J.L. Sessler, P.A. Gale, I. Shin, A synthetic ion transporter that disrupts autophagy and induces apoptosis by perturbing cellular chloride concentrations, Nat. Chem. 9 (2017) 667–675.

[3] a) T. Ito, Y. Xu, S.Y. Kim, R. Nagaishi, T. Kimura, Adsorption behavior and radiation effects of a silica-based (calix(4)+ dodecanol)/SiO2-P adsorbent for selective separation of Cs(I) from high level liquid waste, Separ. Sci. Technol. 51 (2016) 22–31;
b) I. Rais, S. Tachimori, E. Yoo, M. Alexova, M. Bubenikova, Extraction of radioactive Cs and Sr from nitric acid solutions with 25,27-bis(1-octyloxy)calix[4]-26,28-crown-6 and dicyclohexyl-18-crown-6: effect of nature of the organic solvent, Separ. Sci. Technol. 50 (2015) 1202–1212.

[4] a) S. Lee, A.H. Flood, Photoresponsive receptors for binding and releasing anions, J. Phys. Org. Chem. 26 (2013) 79–86;
b) M. Natali, S. Giordani, Molecular switches as photocontrollable "smart" receptors, Chem. Soc. Rev. 41 (2012) 4010–4029.

[5] a) S.S. Deshpande, M.A. Jachak, S.S. Khopkar, G.S. Shankarling, A simple substituted spiropyran acting as a photo reversible switch for the detection of lead (Pb2+) ions, Sensor Actuat. B-Chem. 258 (2018) 648–656;
b) S. Heng, A.M. Mak, R. Kostecki, X. Zhang, J. Pei, D.B. Stubing, H. Ebendorff-Heidepriem, A.D. Abell, Photoswitchable calcium sensor:' On'-'Off' sensing in cells or with microstructured optical fibers, Sensor Actuat. B-Chem. 252 (2017) 965–972.

[6] a) H. Ding, B. Li, S. Pu, G. Liu, D. Jia, Y. Zhou, A fluorescent sensor based on a diarylethene-rhodamine derivative for sequentially detecting Cu^{2+} and arginine and its application in keypad lock, Sensor Actuat. B-Chem. 247 (2017) 26–35;
b) F. Liu, C. Fan, S. Pu, A new "turn-on" fluorescent chemosensor for Zn2+ based on a diarylethene derivative and its practical applications, J. Photochem. Photobiol. A: Chem. 371 (2019) 248–254.

[7] a) A.A. Beharry, G.A. Woolley, Azobenzene photoswitches for biomolecules, Chem. Soc. Rev. 40 (2011) 4422–4437;

b) E. Wagner-Wysiecka, N. Łukasik, J.F. Biernat, E. Luboch, Azo group(s) in selected macrocyclic compounds, J. Incl. Phenom. Macrocycl. Chem. 90 (2018) 189–257.

[8] J. García-Amorós, D. Velasco, Recent advances towards azobenzene-based light-driven real-time information-transmitting materials, Beilstein J. Org. Chem. 8 (2012) 1003–1017.

[9] T. Gao, Y. Xue, Z. Zhang, W. Que, Multi-wavelength optical data processing and recording based on azo-dyes doped organic-inorganic hybrid film, Opt. Express 26 (2018) 4309–4317.

[10] A. Babalhavaeji, G.A. Woolley, Modular design of optically controlled protein affinity reagents, Chem. Comm. 54 (2018) 1591–1594.

[11] L. Stricker, M. Böckmann, T.M. Kirse, N.L. Doltsinis, B.J. Ravoo, Arylazopyrazole photoswitches in aqueous solution: substituent effects, photophysical properties, and host–guest chemistry, Chem. Eur. J. 24 (2018) 8639–8647.

[12] K. Dąbrowa, P. Niedbała, J. Jurczak, Anion-tunable control of thermal Z→E isomerisation in basic azobenzene receptors, Chem. Comm. 50 (2014) 15748–15751.

[13] Y.R. Choi, G.C. Kim, H.-G. Joen, J. Park, W. Namkung, K.-S. Jeong, Azobenzene-based chloride transporters with light-controllable activities, Chem. Comm. 50 (2014) 15305–15308.

[14] J.B. Nanubolu, B. Sridhar, K. Ravikumar, K.D. Sawant, T.A. Naik, L.N. Patkar, S. Cherukuvada, B. Sreedhar, Polymorphism in metformin embonate salt – recurrence of dimeric and tetrameric guanidinium–carboxylate synthons, CrystEngComm 15 (2013) 4448–4464.

[15] J. Bernstein, R.E. Davis, L. Shimoni, N.-L. Chang, Patterns in hydrogen bonding functionality and graph set analysis in crystals, Angew. Chem. Int. Ed. 34 (1995) 1555–1573.

[16] GaussView, Version 5.0.9, Roy Dennington, Todd A. Keith, and John M. Millam, Semichem Inc., Shawnee Mission, KS, (2016).

[17] a) C. Pérez-Casas, A.K. Yatsimirsky, Detailing hydrogen bonding and deprotonation equilibria between anions and urea/thiourea derivatives, J. Org. Chem. 73 (2008) 2275–2284;
b) V. Amendola, G. Bergamaschi, M. Boiocchi, L. Fabbrizzi, M. Milani, The squaramide versus urea contest for anion recognition, Chem. Eur. J. 16 (2010) 4368–4380.

[18] a) A. Sarkar, S. Bhattacharyya, A. Mukherjee, Colorimetric detection of fluoride ions by anthraimidazoledione based sensors in the presence of Cu(II) ions, Dalton Trans. 45 (2016) 1166–1175;
b) E. Wagner-Wysiecka, J. Chojnacki, Chromogenic amides of pyridine-2,6-dicarboxylic acid as anion receptors, Supramol. Chem. 24 (2012) 684–695.

[19] a) K. Alizadeh, B. Rezaei, E. Khazaeli, A new triazene-1-oxide derivative, immobilized on the triacetyl cellulose membrane as an optical Ni^{2+} sensor, Sensor Acuat. B-Chem. 193 (2014) 267–272;
b) N. Łukasik, E. Wagner-Wysiecka, Salicylaldimine-based receptor as a material for iron(III) selective optical sensing, J. Photochem. Photobiol. A-Chem. 346 (2017) 318–326.

[20] a) M. Müri, K.C. Schuermann, L. De Cola, M. Mayor, Shape-switchable azo-macrocycles, Eur. J. Org. Chem. (2009) 2562–2575;
b) N. Łukasik, E. Wagner-Wysiecka, Anion binding by p-aminoazobenzene-derived aromatic amides: spectroscopic and electrochemical studies, Photochem. Photobiol. Sci. 16 (2017) 1570–1579.

[21] K. Dąbrowa, J. Jurczak, Tetra-(meta-butylcarbamoyl)azobenzene: a rationally designed photoswitch with binding affinity for oxoanions in a long-lived Z-state, Org. Lett. 19 (2017) 1378–1381.

[22] STOE, Gmb H. Cie, X-Area 1.75, STOE &Cie GmbH, Darmstadt, Germany, 2015.

[23] G.M. Sheldrick, A short history of SHELX, Acta Cryst. A64 (2008) 112–122.

[24] G.M. Sheldrick, Crystal structure refinement with SHELXL, Acta Cryst. C71 (2015) 3–8.

[25] O.V. Dolomanov, L.J. Bourhis, R.J. Gildea, J.A.K. Howard, H. Puschmann, OLEX2: a complete structure solution, refinement and analysis program, J. Appl. Cryst. 42 (2009) 339–341.

[26] 09 Gaussian, D.01 Revision, M.J. Frisch, G.W. Trucks, H.B. Schlegel, G.E. Scuseria, M.A. Robb, J.R. Cheeseman, G. Scalmani, V. Barone, G.A. Petersson, H. Nakatsuji, X. Li, M. Caricato, A. Marenich, J. Bloino, B.G. Janesko, R. Gomperts, B. Mennucci, H.P. Hratchian, J.V. Ortiz, A.F. Izmaylov, J.L. Sonnenberg, D. Williams-Young, F. Ding, F. Lipparini, F. Egidi, J. Goings, B. Peng, A. Petrone, T. Henderson, D. Ranasinghe, V.G. Zakrzewski, J. Gao, N. Rega, G. Zheng, W. Liang, M. Hada, M. Ehara, K. Toyota, R. Fukuda, J. Hasegawa, M. Ishida, T. Nakajima, Y. Honda, O. Kitao, H. Nakai, T. Vreven, K. Throssell, J.A. Montgomery Jr., J.E. Peralta, F. Ogliaro, M. Bearpark, J.J. Heyd, E. Brothers, K.N. Kudin, V.N. Staroverov, T. Keith, R. Kobayashi, J. Normand, K. Raghavachari, A. Rendell, J.C. Burant, S.S. Iyengar, J. Tomasi, M. Cossi, J.M. Millam, M. Klene, C. Adamo, R. Cammi, J.W. Ochterski, R.L. Martin, K. Morokuma, O. Farkas, J.B. Foresman, D.J. Fox, Gaussian, Inc., Wallingford CT, (2016).

[27] M. Kyvala, I. Lukeš, program package" OPIUM" available (free of charge) at http://www.natur.cuni.cz/~kyvala/opium.html.